6. SITE 510[1]

Shipboard Scientific Party[2]

HOLE 510

Date occupied: November 29, 1979

Date departed: November 30, 1979

Time on hole: 26 hr., 45 min.

Position (latitude; longitude): 1°36.79′N; 86°24.60′W

Water depth (sea level; corrected m, echo-sounding): 2780.8

Water depth (rig floor; corrected m, echo-sounding): 2790.8

Bottom felt (m, drill pipe): 2795.5

Penetration (m): 132.5 (sediment: 111.5; basalt: 21)

Number of cores: 11

Total length of cored section (m): 75.5

Total core recovered (m): 62.96

Core recovery (%): 83

Oldest sediment cored:
Depth sub-bottom (m): 111.5
Nature: Diatom nannofossil ooze
Age: 2.6-3.0 × 10^6 y.
Measured seismic velocity (km/s): 1.52

Basement:
Depth sub-bottom (m): 111.5-132.5
Nature: Basalt
Seismic velocity range (km/s): 5.54-6.03

Principal results: One hole was cored at Site 510. Spot coring was carried out to 67 meters penetration, and from this depth to the basement continuous coring of sediment was done (93-100% recovery). Eighteen meters of basement were penetrated with 27% recovery. The sediments consist of diatom nannofossil oozes throughout. The biogenic silica content of the sediment is higher than at any other of the sites (506-509), and no decrease in silica content occurs at depth. Micropaleontologic evidence suggests that the Pliocene/Pleistocene boundary occurs at 90 meters sub-bottom depth.

Site 510 pore waters have Ca enrichments and Mg depletions up to 15%; extremely high SiO_2 concentrations (up to 1100 μM), reflecting biogenic silica dissolution; and NH_3 and H_2S concentrations that indicate the production of about 400 μM of CO_2 by sulfate reduction.

The basalts recovered at this site differ from those of Sites 506-509. Plagioclase phenocrysts are larger and more abundant, olivine phenocrysts occur, and primary Fe-Ti oxides are only half as abundant as at Sites 506-509. Alteration is also more pervasive than at Sites 506 and 508.

BACKGROUND AND OBJECTIVES

Site 510 is located at 1°36.79′N latitude and 86° 24.60′W longitude in a moderately high heat-flow region (4-5 HFU). The site (Fig. 1) is about 90 km north of the Galapagos Spreading Center and 38 km west-northwest of Leg 54, Site 425. The sediment cover is about 115 meters thick. The site is near magnetic anomaly 2′ and, assuming a 3.25 cm/y. half-spreading rate, the crust should be 2.7 m.y. old.

The main objective of Site 510 was to test the basement drilling capacity of a region of the Galapagos Spreading Center older than the three mounds fields previously studied.

OPERATIONS

Site 510 is located to the north of the Galapagos Spreading Center magnetic anomaly 2′ over crust about 2.7 m.y. old. The *Glomar Challenger* traveled on a course heading of about 344° true from Site 509 beginning at 2048 hours (L), November 28, 1979, with all underway systems on line (12- and 3.5-kHz echo sounding, 5- and 40-in.^{3} air-gun seismic profiling, magnetometer). The exact site was selected over the only relatively flat seafloor and basement, with about 0.15-s reflection time between seafloor and basement (Fig. 2). Several internal reflectors within the sediment column were seen at 0.03, 0.06 (multiple?), and 0.125 s below the seafloor reflection. A beacon was dropped at 0538 hr. (local time) on November 29. After settling over the beacon, the drill string with the conventional rotary drill bit was lowered (0712 to 1430 hr.). No detailed site survey was performed. Site 510 is located on the beacon. We spudded in at 1430 hours, November 29, 1979.

The 115-meter thick sediment column was spot cored, mostly by punch coring through soft sediments without rotation of the bit (Table 1). Intermeshed with the sediment coring program were three *in situ* temperature measurements and pore-water samples at sub-bottom depths of about 38.5 meters, 67 meters, and 95 meters. Hard rock drilling for 9.3 hr. followed, during which the drill bit penetrated 19.0 meters into the basement, while 5.2 meters of basalt were recovered. The bit plugged at 1900 hr. (L), November 29, 1979, after Core 11 was taken, and the core barrel could not be recovered. The drill string was pulled and the site abandoned because of poor drilling conditions in the hole.

---

[1] Honnorez, J., Von Herzen, R. P., et al., *Init. Repts. DSDP*, 70: Washington (U.S. Govt. Printing Office).

[2] Jose Honnorez (Co-Chief Scientist), Rosenstiel School of Marine and Atmospheric Sciences, University of Miami, Miami, Florida; Richard P. Von Herzen (Co-Chief Scientist), Woods Hole Oceanographic Institution, Woods Hole, Massachusetts; Timothy J. Barrett, Mineralogisches Institut, Universitat Tübingen, Tübingen, Federal Republic of Germany (present address: University of Toronto, Toronto, Ontario, Canada); Keir Becker, Marine Physical Laboratory, Scripps Institution of Oceanography, La Jolla, California; Michael L. Bender, Graduate School of Oceanography, University of Rhode Island, Kingston, Rhode Island; Peter E. Borella, Deep Sea Drilling Project, Scripps Institution of Oceanography, La Jolla, California (present address: Saddleback College, Mission Viejo, California); Hans-Wolfgang Hubberten, Institut für Petrographie und Geochemie der Universität Karlsruhe, Federal Republic of Germany; Steven C. Jones, Department of Geology, Florida State University, Tallahassee, Florida (present address: Mobil Oil Company, New Orleans, Louisiana); Shun-ichiro Karato, Ocean Research Institute, University of Tokyo, Tokyo, Japan (present address: The Australian National University, Canberra, Australia); Christine Laverne, Laboratoire de Geologie, Université de l'Ocean Indian, Ste. Clothilde, Réunion, France; Shaul Levi, School of Oceanography, Oregon State University, Corvallis, Oregon; Areg A. Migdisov, Vernadsky Institute of Geochemistry and Analytical Chemistry, USSR Academy of Sciences, Moscow, USSR; S. Anthony Moorby, Department of Geology, Imperial College, London, United Kingdom; Ed L. Schrader, Department of Geology and Geography, University of Alabama, University, Alabama (present address: J. M. Huber Corporation, Macon, Georgia).

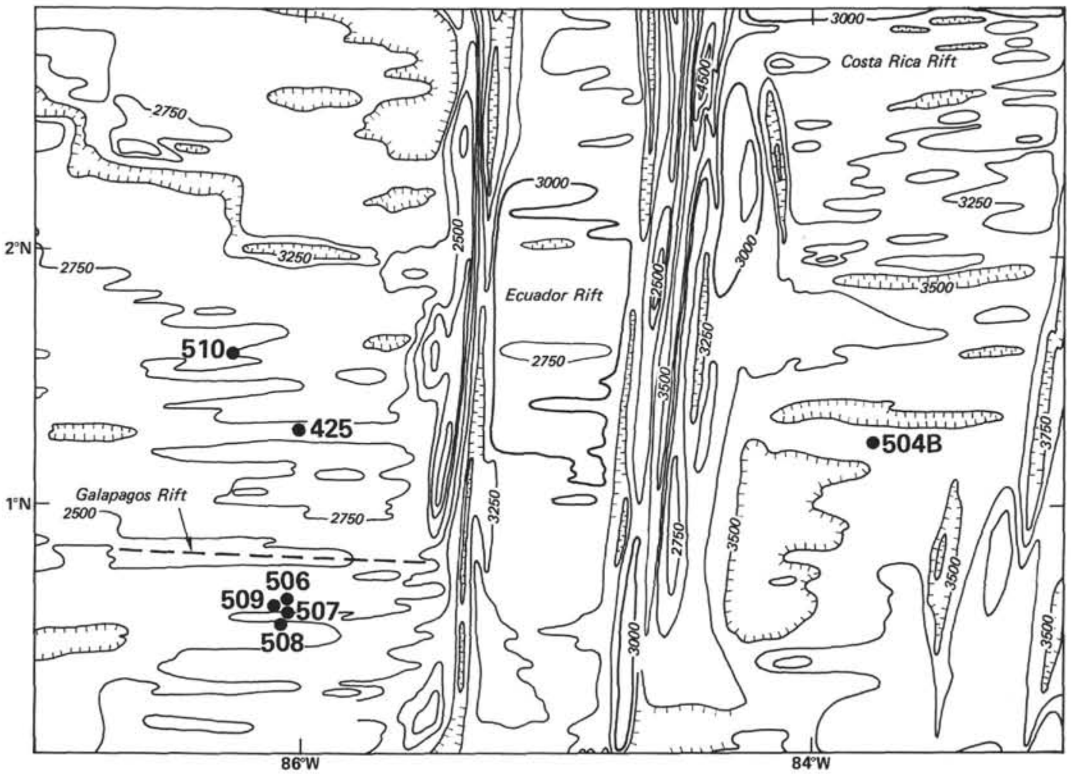

Figure 1. General site locality map, Site 510.

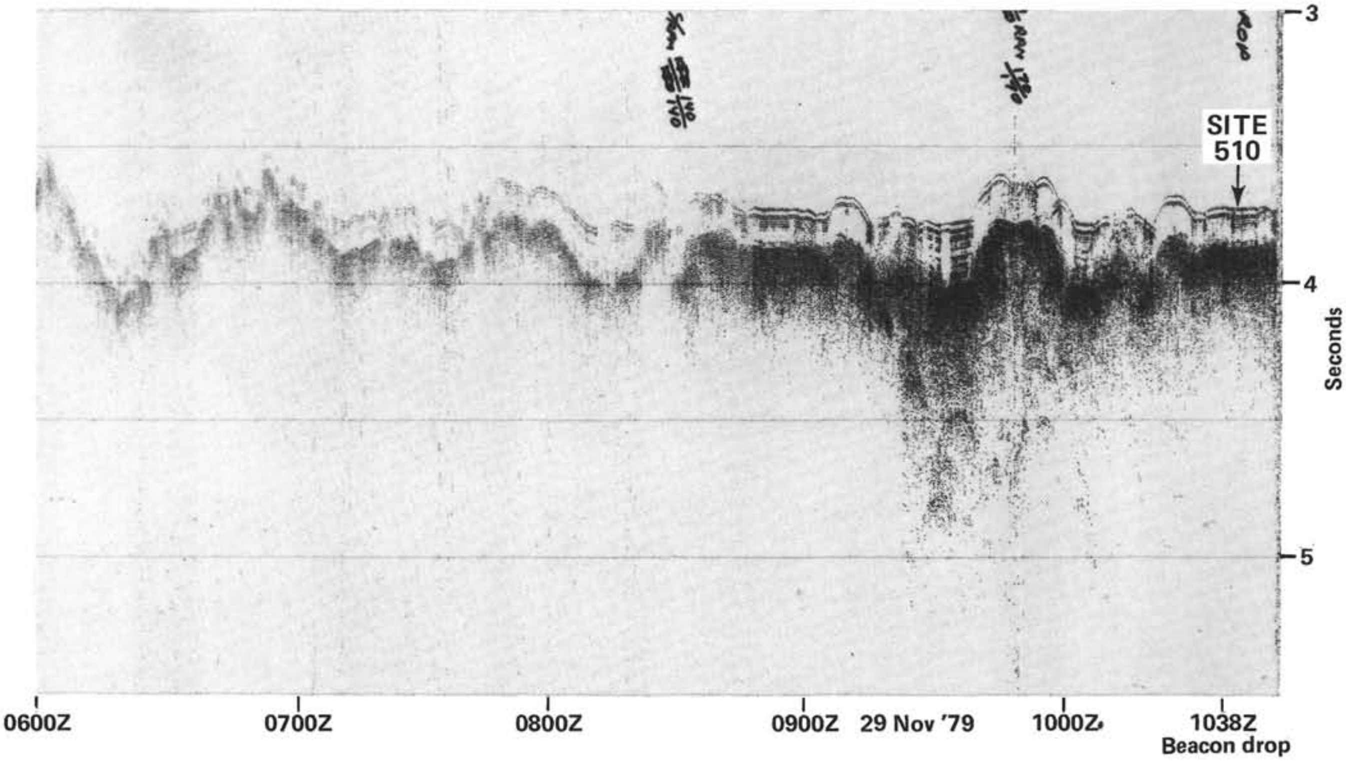

Figure 2. Seismic reflection profile in the vicinity of Site 510. (Horizontal lines spaced at 0.5-s intervals.)

Table 1. Coring summary, Site 510.

Core	Date	Time	Depth from Drill Floor (m) Top Bottom	Depth below Seafloor (m) Top Bottom	Length Cored (m)	Length Recovered (m)	Recovery (%)
1	11/29/79	1414	2795.5-2796.0	0.0-0.5	0.5	0.04	8
HF ISPW	wash	—	2796.0-2834.0	0.5-38.5	—	—	—
2	11/29/79	1741	2834.0-2843.5	38.5-48.0	9.5	8.48	100
HF ISPW	wash	—	2843.5-2862.5	48.0-67.0	—	—	—
3	11/29/79	2116	2862.5-2872.0	67.0-76.5	9.5	9.55	100
4	11/29/79	2221	2872.0-2881.5	76.5-86.0	9.5	9.44	99
5	11/30/79	2323	2881.5-2891.0	86.0-95.5	9.5	9.49	100
6	11/30/79	0151	2891.0-2900.5	95.5-105.0	9.5	9.29	98
7	11/30/79	0259	2900.5-2907.0	105.0-111.5	6.5	9.45	100
8	11/30/79	0456	2907.0-2910.0	111.5-114.5	3.0	2.80	93
9	11/30/79	1119	2910.0-2919.0	114.5-123.0	9.0	3.14	35
10	11/30/79	1404	2919.0-2923.5	123.0-128.0	4.5	0.63	14
11	11/30/79	1659	2923.5-2928.0	128.0-132.5	4.5	0.65	14
				Total:	75.5	62.96	

Work at the site was completed and we were underway to Site 504B at 0341 hr. on December 1, 1979.

SEDIMENT LITHOLOGY AND STRATIGRAPHY

Our primary objective at Site 510 was to drill basement. Consequently, apart from a spot core at the mudline and one between 38.5 meters and 48 meters, only the last 50 meters above the basement (encountered at 111.5 m sub-bottom) were continuously cored (Fig. 3). The sediment throughout consists of a pale olive green (2.5Y 6/2) to light greenish gray (5GY 8/1) diatom nannofossil ooze.

The major and minor constituents of the sediments, determined from smear slides, are: nannofossils, 20-65%; foraminifers, 2-10%; diatoms, 15-50%; unspecified carbonate, tr.-10%; radiolarians, 2-20%; silicoflagellates, tr.-10%; and sponge spicules, tr.-10%.

The sediment between 38.5 meters and 48 meters is lighter in color (light greenish gray) than in the lower 47 meters, where olive green predominates. The upper unit has fewer siliceous microfossils (~20%) than the lower unit (>30%). Throughout the entire hole, diatoms are the most abundant siliceous biogenic component. The higher biogenic silica content of these sediments distinguishes them from pelagic oozes recovered at Sites 506 through 509.

All the recovered rotary drilled cores were highly disturbed. Some sections showed a little mottling, but in only one case (510-2-4, 80 cm) was evidence of burrowing preserved.

Traces of volcanic ash are present throughout the sequence. In Core 7, three thin and highly disturbed ash layers occur (Section 5, 50-60 cm) and Section 6, 20-35 cm and 50-60 cm). The ash in these layers is colorless.

Traces of pyrite occur in most cores below 67 meters. When split, all cores from this depth to the basement smelled of H_2S, indicating that reducing conditions are present throughout this interval. No induration of the sediments immediately overlying basement was observed.

BIOSTRATIGRAPHY

Since our primary objective was to recover basement material, conventional drilling techniques were used to penetrate the overlying sediments. In the top 67 meters of sediment, spot cores were taken only between 0.0 to 0.5 meters and 38.5 to 48.0 meters. Below 67 meters the sediments were continuously cored until basement was reached.

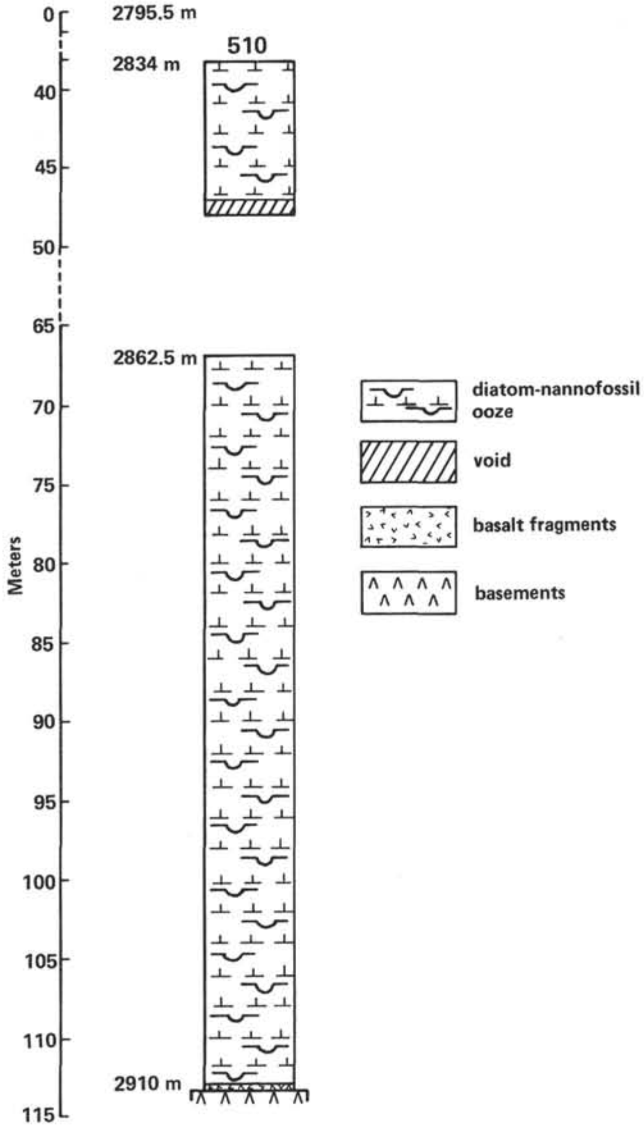

Figure 3. Lithostratigraphic summary, Site 510.

A sample from the core catcher of each core was examined for calcareous nannofossils, foraminifers, diatoms, radiolarians, and silicoflagellates in order to determine their abundance (see core description). Calcareous nannofossils and planktonic foraminifers were used for age determinations. Ages determined by the use of calcareous nannofossils are based on the standard calcareous nannoplankton zonation by Martini (1971) and the revised zonation of the Pleistocene by Gartner (1977). The occurrence of *Discoaster brouweri, Reticulofenestra pseudoumbilica*, and *Ceratolithus rugosus* in the basal sediments indicate an early Pliocene age (*Reticulofenestra pseudoumbilica* Zone, 2.6 to 3.0 Ma). The presence of the planktonic foraminifers *Globigerinoides fistulosus, G. extremus*, and *G. obliquus* support the early Pliocene age. The Pliocene/Pleistocene boundary is located approximately 75 meters sub-bottom.

Calcareous Nannofossils

Calcareous nannofossils are abundant and moderately preserved throughout the section. The core-catcher samples are assigned to the following zones: Core 1—*Emiliania huxleyi* Zone, Core 2—*Gephyrocapsa oceanica* Zone, Core 3—*Pseudoemiliania lacunosa* Zone, Core 4—*Helicopontosphaera selli* Zone, Cores 5 and 6—*Discoaster brouweri* Zone, Core 7—*Reticulofenestra pseudoumbilica* Zone.

Calcareous nannofossils in the basal sediments include, *D. brouweri* (common), *R. pseudoumbilica* (few), *Ceratolithus rugosus* (rare), *H. kamptneri* (common), and *Cyclococcolithina leptopora* (common).

Planktonic Foraminifers

Planktonic foraminifers are common and moderately preserved in Cores 1 through 5. Foraminifers in Cores 6 and 7 are poorly preserved and reduced in number. Selective dissolution of the planktonic foraminifers had artificially increased the percentage of benthic foraminifers in these cores. The basal assemblage of foraminifers includes: *Globorotalia dutertrei* (common), *G. tosaensis* (rare), *G. scitula* (few), *G. tumida* (few), *Globigerinoides fistulosus* (rare), *G. obliquus* (rare), *G. extremus* (rare), *Sphaeroidinella dehiscens* (rare), and *Pulleniatina obliquiloculata* (few). The majority of the planktonic foraminifers are warm-water tropical to subtropical forms.

X-RAY DIFFRACTION ANALYSIS

The results of the X-ray diffraction analysis for Site 510 are given in Table 2.

Two samples of gray volcanic ash were analyzed from Core 7, Section 5. Volcanic glass was positively identified from smear slides along with minor calcareous components. Calcite was the only mineral identified by X-ray diffraction.

SEDIMENTATION RATES

Table 3 summarizes the sedimentation and accumulation rates estimated from ages based on paleontologic and paleomagnetic data. The rate estimates agree well between the two methods. At previous sites the paleontologic age (age of lowermost sediments) and the magnetic age (age of crust) did not agree. This discrepancy may result from an incomplete biostratigraphic record at the previous sites (506–509) caused by nondeposition, poor preservation, or lack of biostratigraphic control in areas of very thin sediment cover.

Table 2. X-ray diffraction analysis, Site 510.

Sample (interval in cm)	Mineral	Major Peak 2θ	d(Å) (uncorr.)	Major Peak 2θ	d(Å) (corr.)
510-7-5, 33–34		32.4	2.76	32.6	2.75
	Halite	31.3	2.86	31.5	2.84
	Sylvite	28.1	3.18	28.3	3.15
	(std. spike)	25.25	3.53	25.45	3.50
510-7-5, 58–59	Calcite	39.2	2.30	39.5	2.28
	Calcite	35.55	2.52	35.85	2.51
	Halite	31.5	2.84	31.8	2.81
	Calcite	29.2	3.06	29.5	3.03
	Sylvite	28.0	3.19	28.3	3.15
	(std. spike)	25.8	3.45	26.1	3.41
	Calcite	22.8	3.90	23.1	3.85
		11.9	7.43	12.10	7.31

Table 3. Sedimentation rates, Site 510.

Hole	S^a (m)	Sedimentation Rate (cm/10^3 y.)		P^b (%)	Sediment Accumulation Rate (cm/10^3 y.)		Average Grain Density (g/cm^3)	Accumulation Rate (g/cm^2/10^3 y.)	
		A	B		A	B		A	B
510	114.5	3.81 4.40	4.19	79.37	0.79 0.91	.865	2.55	2.32 2.01	2.20

Note: Columns lettered "A" show, respectively, minimum and maximum values based on paleontological evidence. Paleontological evidence places the estimated age at the bottom of each hole at 2.6 to 3 × 10^6 y. Spreading rates (columns lettered "B") are based on an estimated age of 2.73 m.y.

[a] S = Sediment thickness (recorded drilling thickness).

[b] P = Porosity (fractional void space) ± (void space)/(total volume); values are averages taken from the Physical Properties section.

PORE-WATER GEOCHEMISTRY

Pore-water results are presented in Tables 4 and 5, and Figure 4. Three *in situ* samples were collected. The *in situ* chemistry agrees well with centrifuge-sample chemistry except that centrifuge Ca concentrations are approximately 0.5 mM less than *in situ* Ca concentrations (see Site 509 pore-water summary).

In pore waters from Site 510, the signal for diagenesis of biogenic debris is larger than in any of the Galapagos mounds area holes. NH_3 concentrations rise to about 60–70 μM. Measured H_2S concentrations are erratic, probably as a result of partial oxidation before or during pore-water sampling, but reach 360 μM. These constituents undoubtedly record SO_4^{2-} reduction by organic matter according to the following reaction:

$$(CH_2O)_{106}\,(NH_3)_{16}\,(H_3PO_4) + 53SO_4^{2-}$$
$$\rightarrow 106HCO_3^- + 16NH_3 + H_3PO_4 + 53H_2S$$

Table 4. Shipboard pore-water data, Site 510.

Core Section	ISPW No.	Sub-bottom Depth (m)	SiO_2 (μM)	NH_3 (μM)	S^{2-} (μM)	Ca^{2+} (mM)	Mg^{2+} (mM)	Cl (‰)	S (‰)
2-1	161	39.89–40.00	850	38	140	10.88	53.63	19.34	35.5
2-5	162	45.89–46.00	820	45	130	10.75	53.58	19.34	35.8
3-1	163	68.89–69.00	960	59	230	11.32	53.26	19.47	36.0
3-5	164	14.89–75.00							
4-2	165	79.39–79.50	1060	63	180	10.90	52.55	19.34	35.5
4-5	166	83-89–84.00							
5-2	167	88.89–89.00	1090	67	130	11.22	51.65	19.38	35.8
5-5	168	93.39–93.50	1110	63					
6-2	169	98.39–98.50	1110	63	360	11.24	51.68	19.24	35.8
6-5	170	102.89–103.00	1120	63	250				
7-2	171	107.89–128.00	1130	55		12.25	50.79	19.21	35.8
7-5	172	112.39–112.50	1040	49	140	11.89	50.50	19.18	35.8

Table 5. Shipboard pore-water data for *in situ* samples, Site 510.

Sample	Sub-bottom Depth (m)	SiO_2 (μM)	Ca^{2+} (mM)	Mg^{2+} (mM)	Cl (‰)	S (‰)
1W 158	38.5	730				
1SPW #14			11.30	52.48	19.24	35.2
1W 159	67	1050	11.77	53.04	19.31	35.8
1SPW #15						
1W 160	96	1090	11.92	51.62	19.18	35.5
1SPW #16						

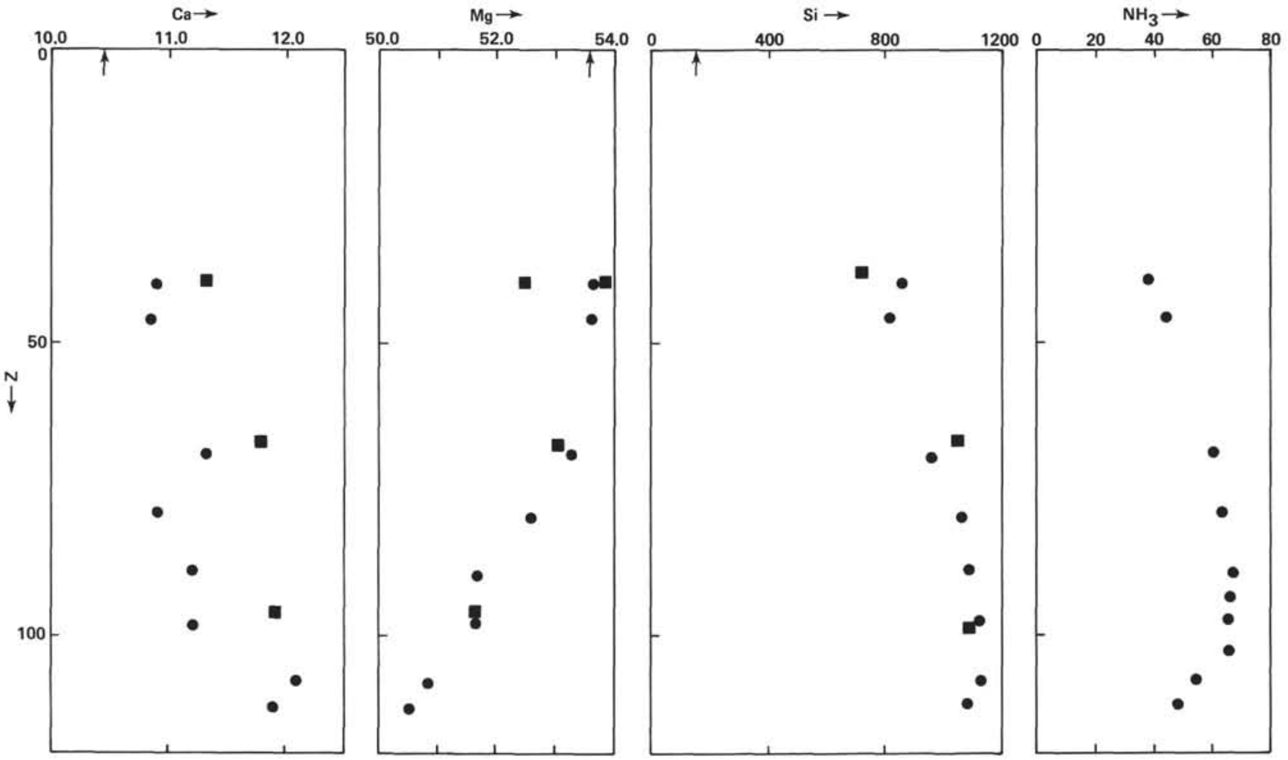

Figure 4. Site 510 pore-water chemistry. (Ca, Mg in mM/l, Si, NH_3 in μM/l. Circles are centrifuge samples; squares are Barnes *in situ* samples. Arrows indicate bottom water concentrations.)

It is not possible to infer the metabolic CO_2 content of the pore waters from the NH_3 and H_2S data, since both chemicals may be incorporated into solids (NH_3 may go into clay mineral ion-exchange positions and S^{2-} may form iron sulfides).

SiO_2 concentrations reach high levels—about 1100 μM. The source of this Si is undoubtedly dissolution of the biogenic silica making up about half the sediment.

Calcium concentrations increase downhole and magnesium concentrations decrease. The gradients are greatest in the lower part of the hole and clearly imply coupled downhole Mg diffusion and uphole Ca diffusion, as the result of seawater–basalt reactions in the basement. The magnesium-depth profile shows the Mg gradient to be much greater at depth than in the top part of the sediment, and thus cannot be explained by simple magnesium diffusion from seawater to basalt through sediments having a constant diffusion rate. The shape of the magnesium profile may be explained by the following hypotheses (none of which appears particularly attractive): nonsteady-state conditions in the pore waters; diffusion coefficients in the bottom half of the hole an order of magnitude lower than in the upper half of the hole; occurrence at 40 to 60-meter depths of reactions in the sediments which produce magnesium and consume calcium; extremely slow advection down through the sediment (on the order of 0.05 cm $y.^{-1}$). The last possibility is favored, but it is untestable.

PHYSICAL PROPERTIES

The wet-bulk density of sediments from this site ranges from 1.24 to 1.49 g/cm^3, porosity from 71.5 to 84.5%, sonic velocity from 1.49 to 1.54 km/s, and thermal conductivity from 0.79 to 1.08 W/m•K.

The depth gradients of physical properties are very small down to 80 meters sub-bottom depth, becoming larger in the deeper part of the sedimentary layer (80 to 110 m).

The drilled thickness of sediments (115 m), combined with the observed seismic-reflection delay of the basement's reflection behind the bottom reflection (0.150 ± 0.005 s), give an average sound velocity of 1.53 ± 0.07 km/s through the sediment column. The deepest seismic reflection above basement (0.125 s) may correspond to the increased gradients in physical properties a few tens of meters above basement.

HEAT FLOW

Three lowerings of the temperature probe were made at Site 510, to sub-bottom depths of 39½ meters, 67 meters, and 95½ meters. The observed temperature gradient was fairly linear. Since the thermal conductivity data (Karato and Becker, this volume) was better fit by a mean value than an increase with depth, the temperature gradient was taken to be the best linear fit to the temperature data, 0.22°/m.

Using the average conductivity value of 0.89 Wm^{-1} K^{-1}, we obtain a heat-flow value of 190 mW/m^2. Judging from the linearity of temperature vs. depth, the heat flow at this site is nearly all conductive, which is not unexpected since the sediment cover (~115 m) may be sufficiently thick to close off convective exchange between the basement pore water and the bottom water. (See Becker et al., this volume.)

IGNEOUS PETROLOGY AND LITHOSTRATIGRAPHY

At Site 510, 21 meters of igneous rock were cored with 6 meters recovered (29% recovery). Recovery and initial penetration were better than at previous Galapagos sites; however, after 21 meters of penetration, hole conditions deteriorated and drilling was halted.

Although only one lithostratigraphic unit of medium-grained, moderately plagioclase phyric basalt was recognized within this rock unit, 11 separate cooling units were tentatively defined on the basis of textural criteria (such as glassy rinds, vesiculation, and grain-size variation, Table 6). The multiplicity of cooling units may be the result of our having cored a sequence of very thin flows or a pillow basalt unit. Although alteration of the basalt will be described in a following section, it should be noted that some phenocrysts megascopically appeared to be clinopyroxene, though in thin sections they were seen to be smectite pseudomorphs after olivine. Thus, these basalts might also be classified as sparsely olivine phyric. Site 510, then, was the only Galapagos site of Leg 70 to contain basalt with substantial quantities of olivine phenocrysts.

Vesicles are generally rare to absent, but they do occur in areas of finer-grained texture and in glassy rinds. Interiors of the pillows (or flows) are essentially free of vesicles.

Many of the basalt pieces are angular to subangular, nearly equant, and thus unorientable. Additionally, alteration rinds often parallel surfaces on these cobble-sized pieces. The rubble-like nature of these samples is consistent with a sequence of cored basalt pillows.

In thin section, the basalts are medium-grained, hyalopilitic to variolitic with plagioclase (2.1 mm) and olivine (0.8 × 0.6 mm) phenocrysts. The interstitial material in the hyalopilitic textural group has quenched to variolites of plumose or sheaf textures composed of intergrown plagioclase and clinopyroxene. A few fresh olivines were observed; however, most of the olivine phenocrysts were replaced by smectite and iddingsite(?). Samples from the variolitic textural group displayed plagioclase phenocryst laths and skeletal plagioclase laths, serving as sites for preferred nucleation of microlites. Vesicles and voids are rare in both textural groups, but when they occur are often filled with green smectite.

Titanomagnetite is less abundant in Site 510 basalts than at previous Leg 70 Galapagos sites (ranging from 3 to 8% at Site 510). The sizes of these crystals all average less than 20 µm in diameter or across the longest axis. The magnetites are skeletal to anhedral in morphology. Primary sulfide spheres of pyrrhotite and chalcopyrite compose less than 1% of the rock and are commonly less than 5 µm in diameter. Secondary pyrite occurs as grains in glassy areas and as vein fillings with smectite. These secondary sulfides compose as much as 3% of some thin sections. In one sample (Sample 510-9-1, 50-52 cm), chalcopyrite occurs as a bleb or anhedral crystal in secondary pyrite replacing mesostasis.

Basement Alteration

Megascopically, most of the pieces are surrounded by a thin (<0.5 mm) coating of green, blue, and yellow-brown material. On the sawn surfaces, a thick (5-40 mm) altered rim occurs, which is darker than the fresh core of the pieces. Alteration also appears to be controlled by cracks, fissures, and exposed surfaces. Vesicles and more frequent voids seem empty or, more often, filled by blue and green clay.

Microscopic examination shows that these vesicles and miarolitic voids are coated and sometimes filled by different kinds of smectite and more sparsely by calcite and pyrite. The following paragenetic succession from the rock interior through an alteration rim was observed adjacent to a smectite veinlet: (1) orange-brown smectite(?) with iron oxyhydroxides, (2) mixed orange-brown and green smectites (and possible calcite), (3) green smectite, and (4) very light-brown smectite.

Cracks are generally filled by green smectite. In some areas, smectite seems to replace glass. In the glassy rim of Sample 510-11-1, 40-43 cm, the formation of fibropalagonite from the glass (devitrification process) on each side of a smectite vein has been observed. Finally, olivine crystals are clearly replaced by different kinds of smectite, which are orange brown, green, or very light brown, according to the zone where olivine crystals occur.

Thus, the alteration of the basalts from Site 510 chiefly differs from that of Sites 506, 507, and 508 in the thickness of the altered rim, which can be explained by a longer interaction of basalts with seawater. Smectite is the most common mineral, with calcite and pyrite oc-

Table 6. Cooling units, Site 510.

Unit	Depth (m)	Piece No.	Lithology
1	114.5-114.95	53-57	Medium-grained moderately to highly plagioclase phyric basalt
2	114.95-115.10	58-59	Fine-grained aphyric basalt
3	115.10-116.10	60-70	Medium-grained moderately to highly plagioclase phyric basalt
4	116.10-116.65	71-79	Fine-grained moderately plagioclase clinopyroxene phyric basalt
5	116.65-117.95	80-97	Fine- to medium-grained moderately plagioclase clinopyroxene phyric basalt
6	117.95-118.05	98-99	Fine-grained moderately plagioclase phyric basalt
7	118.05-118.35	100-106	Medium-grained moderately plagioclase phyric basalt
8	123.5-124.4	107-117	Fine-grained aphyric to plagioclase clinopyroxene phyric basalt
9	128.0-128.3	118-122	Medium-grained moderately plagioclase phyric basalt
10	128.3-128.4	123	Fine-grained moderately plagioclase phyric basalt
11	128.4-129.0	124-133	Medium-grained moderately plagioclase phyric basalt

curring less frequently. As at previous sites, this type of alteration is the result of low temperature weathering.

PHYSICAL PROPERTIES (BASEMENT)

Physical properties of six samples were measured. Wet-bulk density ranges from 2.91 to 2.96 g/cm^3, porosity from 2.7 to 5.0%, sonic velocity from 5.53 to 5.85 km/s. Basalts from Site 510 have higher sonic velocity than do those from Sites 506, 507, 508. This probably results from the difference in their grain density (3.00 g/cm^3 for Site 510; 3.05 g/cm^3 for Sites 506, 507, and 508).

BASEMENT PALEOMAGNETISM

Site 510 is about 89 km north of the Galapagos Spreading Center, on basement whose age is approximately 2.73 × 10^6 years, based on a half-spreading rate of 3.25 cm/y. (Sclater and Klitgord, 1973). Basement penetration and recovery at Site 510 were only a little better than at Sites 506, 507, and 508. Seventeen oriented plus one unoriented minicore were sampled for shipboard paleomagnetic studies. The paleomagnetic measurements and the discussions associated with the results are essentially identical to those of Site 506. The uncertainties below, associated with the values of the magnetic parameters, represent one standard deviation.

$J_{NRM} = 6 \pm 4 \times 10^{-3}$ gauss (G). This value is less than one-third of the value at Sites 506–508. This decrease in J_{NRM} may be the result, in part, of progressive low-temperature oxidation of the titanomagnetites. However, the decrease in J_{NRM} may also be related to a decrease in total iron content at Site 510. This is suggested by the more common occurrence of olivine phenocrysts in thin sections from Site 510 than from Sites 506–508. Furthermore, preliminary observations of the opaques while on board the *Glomar Challenger* indicated a lesser abundance of titanomagnetite grains at Site 510 than at Sites 506–508. Thus, it might be that Site 510 is just outside the region of unusually high-amplitude magnetic anomalies. For example, if

$$\overline{\chi} = 0.97 \pm 0.35 \times 10^{-3} \text{ G/Oe},$$

then $\overline{Q} = 22 \pm 14$, illustrating the dominance of the remanence relative to induced magnetization and consistent with the distinct magnetic anomalies observed in this region.

Relatively high stability of the remanence is indicated by stepwise AF demagnetizations having median peak demagnetization fields ranging from 111 to 373 Oe with a mean of 180 Oe. All the stable inclination values are more negative than the NRM inclinations. This is consistent with removal during AF demagnetization of a component of viscous remanent magnetization acquired in the recent geomagnetic field, whose inclination at Site 510 is about +20°. However, only small changes in the magnetization directions are observed during AF demagnetization. The mean stable inclination is $-16° \pm 4°$; this small dispersion of the stable inclinations suggests that the basalts cored at Site 510 probably represent a relatively short volcanic episode. Furthermore, the shallow inclinations at Site 510 are in line with the equatorial latitude of the site.

PRINCIPAL RESULTS

Only one hole was cored at Site 510. Spot coring was carried out to 67 meters penetration, and from this depth to the basement continuous coring of sediment was done (93–100% recovery). Eighteen meters of basement were penetrated with 27% recovery. The sediments consist of diatom nannofossil oozes throughout. The biogenic silica content of the sediment is higher than at any other of the sites (506–509), and no decrease in silica content occurs at depth. Micropaleontologic evidence suggests that the Pliocene/Pleistocene boundary occurs at 90 meters sub-bottom depth.

The basalts recovered at this site differ from those of Sites 506–509. Plagioclase phenocrysts are larger and more abundant; olivine phenocrysts occur and primary Fe–Ti oxides are only about half as abundant as at Sites 506–509. Alteration is also more pervasive than at Sites 506 and 508.

REFERENCES

Gartner, S., 1977. Calcareous nannofossil biostratigraphy and revised zonation of the Pleistocene. *Mar. Micropaleontol.*, 2:1–25.

Klitgord, K. D., and Mudie, J. D., 1974. The Galapagos Spreading Center: A near bottom geophysical survey. *Geophys. J. R. Astron. Soc.*, 38:563–586.

Martini, E., 1971. Standard Tertiary and Quaternary calcareous nannoplankton zonation. *In* Farinacci, A. (Ed.), *Second Planktonic Conf. Proc.:* Rome (Tecnoscienza), pp. 739–785.

Sclater, J. G., and Klitgord, K. D., 1973. A detailed heat flow, topographic and magnetic survey across the Galapagos Spreading Center at 86°W. *J. Geophys. Res.*, 78:6951–6975.

---

[3] $Q = J_{NRM}/\chi H$, where χ is the low-field susceptibility and H ≈ 0.33 Oe is the intensity of the geomagnetic field at the sampling site.

SITE 510 HOLE CORE 1 CORED INTERVAL 0.0–0.5 m

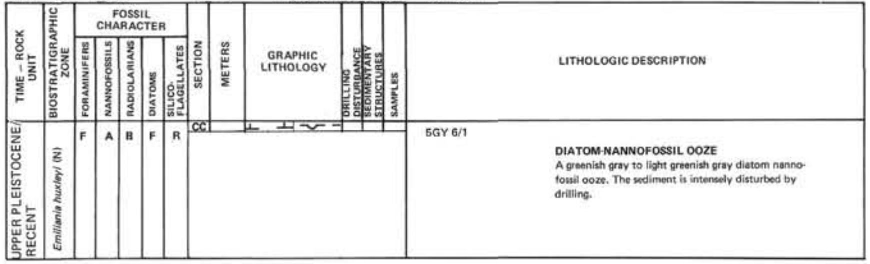

DIATOM-NANNOFOSSIL OOZE

A greenish gray to light greenish gray diatom nannofossil ooze. The sediment is intensely disturbed by drilling.

SITE 510 HOLE CORE 2 CORED INTERVAL 38.5–48.0 m

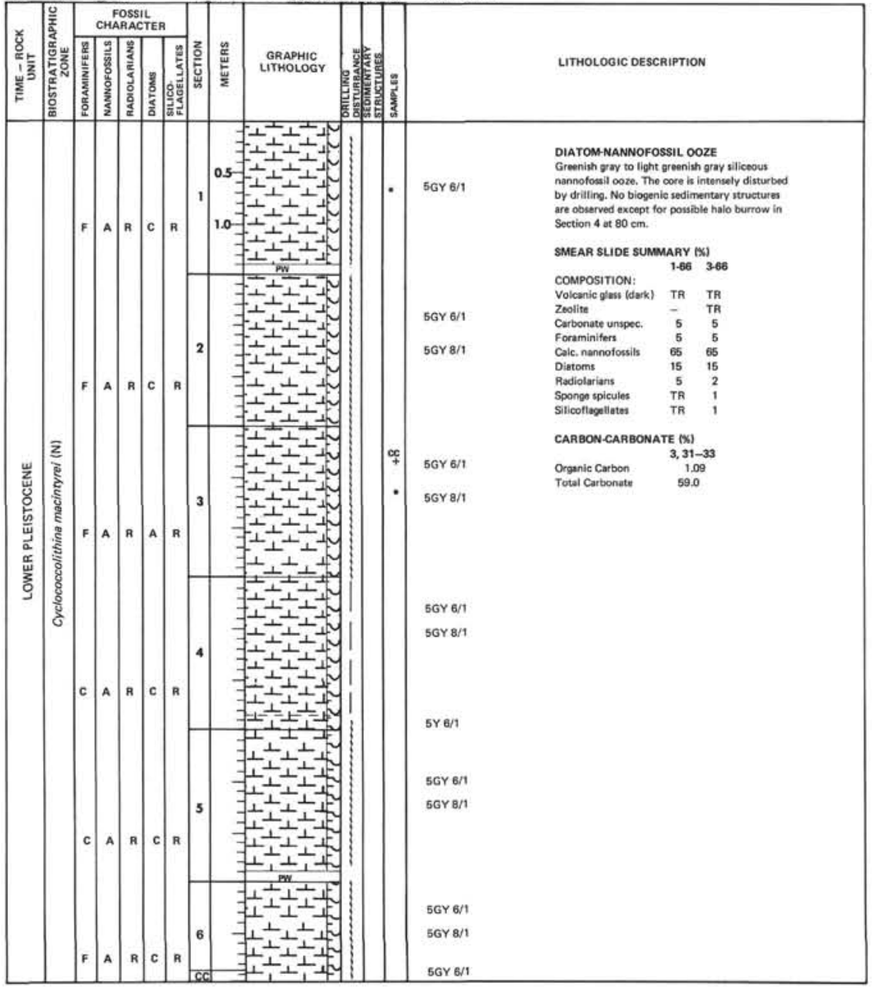

DIATOM-NANNOFOSSIL OOZE

Greenish gray to light greenish gray siliceous nannofossil ooze. The core is intensely disturbed by drilling. No biogenic sedimentary structures are observed except for possible halo burrow in Section 4 at 80 cm.

SMEAR SLIDE SUMMARY (%)

	1-66	3-66
COMPOSITION:		
Volcanic glass (dark)	TR	TR
Zeolite	–	TR
Carbonate unspec.	5	5
Foraminifers	5	5
Calc. nannofossils	65	65
Diatoms	15	15
Radiolarians	5	2
Sponge spicules	TR	1
Silicoflagellates	TR	1

CARBON-CARBONATE (%)

	3, 31–33
Organic Carbon	1.09
Total Carbonate	59.0

SITE 510 HOLE CORE 3 CORED INTERVAL 67.0–76.5 m

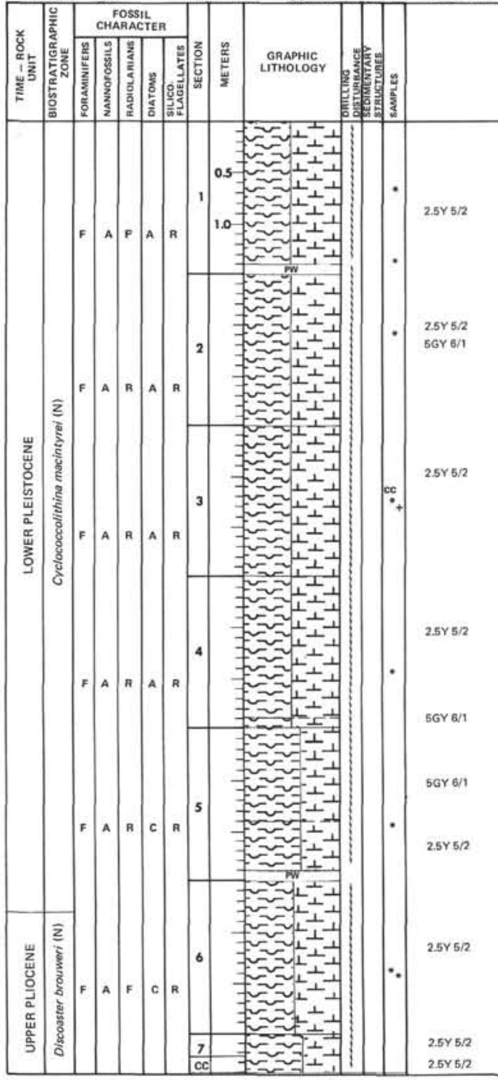

LITHOLOGIC DESCRIPTION

DIATOM-NANNOFOSSIL OOZE

Middle to pale olive green to greenish gray diatom nannofossil ooze. There are possibly some mottling and biogenic structures but the high degree of drilling disturbance has destroyed much of the detail. A strong smell of H_2S occurred when each section was split.

SMEAR SLIDE SUMMARY (%)

	1-62	1-136	2-63	3-64	4-90	5-90	6-85	6-90
COMPOSITION:								
Pyrite	TR	1	–	–	1	–	–	–
Heavy minerals	–	–	–	TR	–	–	–	–
Clay minerals	TR	–	–	–	TR	–	–	–
Volcanic glass (light)	TR	–	–	–	–	TR	–	–
Carbonate unspec.	5	–	–	–	5	–	–	10
Foraminifers	3	5	5	5	3	5	5	5
Calc. nannofossils	60	30	40	30	60	25	20	35
Diatoms	20	50	35	40	25	45	40	30
Radiolarians	10	10	10	10	15	20	20	15
Sponge spicules	2	–	–	–	3	–	5	5
Silicoflagellates	1	5	10	10	TR	5	10	TR
Discoasters	–	–	–	–	TR	TR	–	–

CARBON-CARBONATE (%)

	3, 73–75
Organic Carbon	2.15
Total Carbonate	40.0

SITE 510 HOLE CORE 4 CORED INTERVAL 76.5–86.0 m

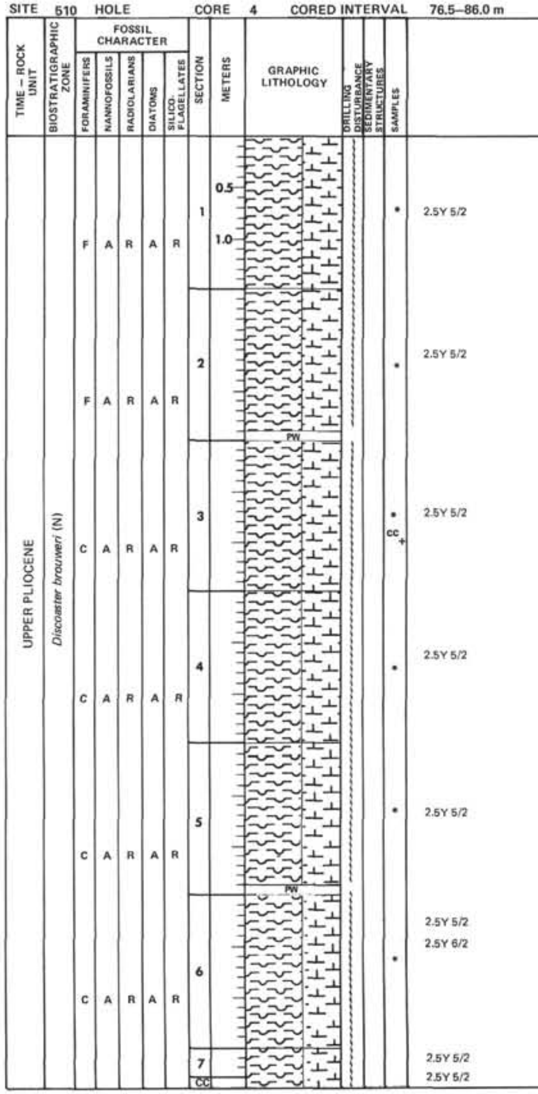

LITHOLOGIC DESCRIPTION

DIATOM-NANNOFOSSIL OOZE

A pale olive green diatom-nannofossil ooze. Very little mottling and no biogenic sedimentary structures are observed. Much of the detail is destroyed by intense drilling disturbance. A strong odor of H_2S occurred when each core was split.

SMEAR SLIDE SUMMARY (%)

	1-71	2-71	3-71	4-65	5-66	6-62
COMPOSITION:						
Pyrite	–	–	–	–	–	1
Volcanic glass (light)	TR	–	TR	TR	–	–
Zeolite	–	–	–	TR	–	TR
Micronodules	–	–	–	TR	–	–
Carbonate unspec.	5	10	10	5	3	5
Foraminifers	5	5	5	2	2	2
Calc. nannofossils	35	50	40	35	30	40
Diatoms	30	20	30	45	35	40
Radiolarians	15	10	8	5	15	5
Sponge spicules	8	5	–	2	–	5
Fish debris	2	1	2	–	–	–
Silicoflagellates	TR	1	5	5	15	2
Discoasters	–	TR	–	–	–	TR

CARBON-CARBONATE (%)

	3, 93–95
Organic Carbon	2.69
Total Carbonate	37.0

SITE 510 HOLE CORE 5 CORED INTERVAL 86.0–95.5 m

TIME – ROCK UNIT	BIOSTRATIGRAPHIC ZONE	FOSSIL CHARACTER FORAMINIFERS	NANNOFOSSILS	RADIOLARIANS	DIATOMS	SILICO-FLAGELLATES	SECTION	METERS	LITHOLOGIC DESCRIPTION
UPPER PLIOCENE	*Discoaster brouweri* (N)	F	A	F	A	R	1	0.5 1.0	2.5Y 5/2
		C	A	C	A	R	2		2.5Y 5/2
		C	A	F	A	R	3		2.5Y 5/2 2.5Y 5/2
		C	A	F	A	R	4		2.5Y 6/2
		F	A	R	C	R	5		2.5Y 6/2
		F	A	F	C	R	6		2.5Y 6/2
							7		2.5Y 6/2
							CC		2.5Y 6/2

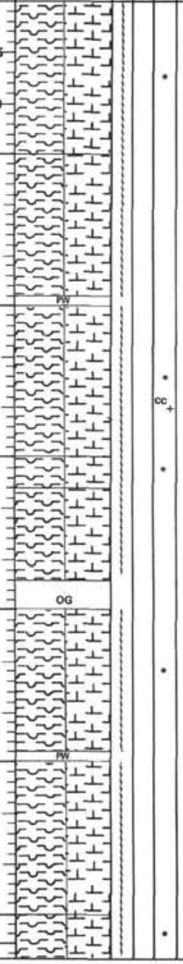

DIATOM-NANNOFOSSIL OOZE

Olive green diatom-nannofossil ooze. No mottling or bioturbation is observed. The strong odor of H_2S was detected when each section was split. Intense drilling disturbance occurs throughout the core.

SMEAR SLIDE SUMMARY (%)

	1-79	3-79	4-20	5-60	7-22
COMPOSITION:					
Quartz	–	–	–	TR	–
Feldspar	–	–	TR	–	–
Heavy minerals	–	–	2	–	–
Clay minerals	–	3	–	5	–
Volcanic glass (light)	–	TR	TR	–	–
Carbonate unspec.	3	2	3	5	–
Foraminifers	5	5	2	2	TR
Calc. nannofossils	40	30	45	50	35
Diatoms	40	30	30	30	35
Radiolarians	10	15	10	5	TR
Sponge spicules	5	5	5	3	15
Silicoflagellates	1	3	2	2	10
Discoasters	–	TR	–	–	TR

CARBON-CARBONATE (%)

	3, 93–95
Organic Carbon	3.24
Total Carbonate	41.0

SITE 510 HOLE CORE 6 CORED INTERVAL 95.5–105.0 m

TIME – ROCK UNIT	BIOSTRATIGRAPHIC ZONE	FOSSIL CHARACTER FORAMINIFERS	NANNOFOSSILS	RADIOLARIANS	DIATOMS	SILICO-FLAGELLATES	SECTION	METERS	LITHOLOGIC DESCRIPTION
UPPER PLIOCENE	*Discoaster brouweri* (N)	F	A	F	C	R	1	0.5 1.0	2.5Y 6/2
		F	A	F	C	R	2		2.5Y 6/1 2.5Y 5/2
		F	A	F	C	R	3		2.5Y 6/1
		F	A	F	C	R	4		5GY 6/1
		F	A	F	A	R	5		5GY 6/1
		F	A	F	A	R	6		5GY 6/1
							7		5GY 6/1
							CC		5GY 6/1

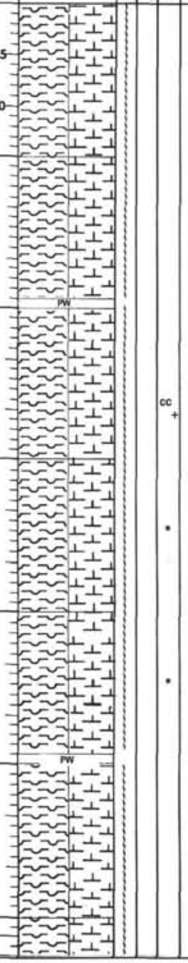

DIATOM-NANNOFOSSIL OOZE

Light greenish gray to light olive green diatom-nannofossil ooze. Some mottling but highly disturbed by drilling. A strong odor of H_2S was detected when each section was split.

SMEAR SLIDE SUMMARY (%)

	4-70	5-70
COMPOSITION:		
Pyrite	TR	TR
Volcanic glass (light)	–	TR
Carbonate unspec.	5	5
Foraminifers	3	5
Calc. nannofossils	45	35
Diatoms	35	35
Radiolarians	5	15
Sponge spicules	5	2
Fish debris	–	TR
Silicoflagellates	TR	TR
Discoasters	2	3

CARBON-CARBONATE (%)

	3, 93–95
Organic Carbon	1.86
Total Carbonate	64.0

SITE 510 HOLE CORE 7 CORED INTERVAL 105.0–111.5 m

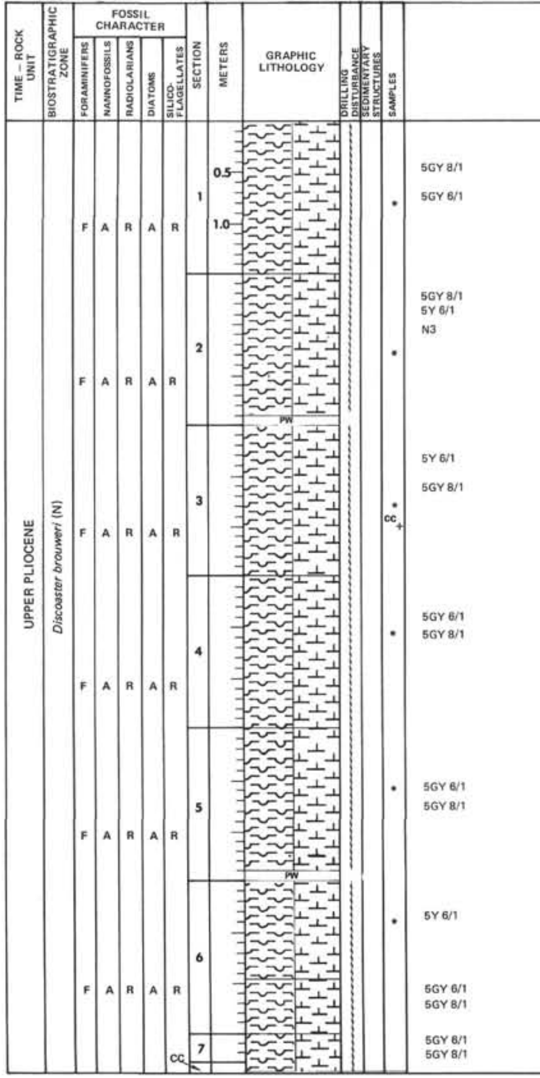

LITHOLOGIC DESCRIPTION

DIATOM-NANNOFOSSIL OOZE

Light greenish gray to light olive gray diatom-nannofossil ooze. Some deformed wisps of dark gray material are present throughout Section 2. Three thin ash layers occur; Section 5, 50–60 cm, Section 6, 20–35 cm and 50–60 cm. The layers were probably about 1 cm thick but are very deformed by the high degree of drilling disturbance. No biogenic sedimentary structures are visible. There was an odor of H_2S when each section was split.

Note: Only 6 m penetration was recorded for this core. The top 3.5 m of the core may therefore represent a repetition of the sequence due to caving in of the hole.

SMEAR SLIDE SUMMARY (%)

	1-80	2-80	3-80	4-57	5-57 (M)	6-35 (M)
COMPOSITION:						
Clay minerals	2	2	3	3	–	–
Volcanic glass (light)	–	TR	–	TR	90	90
Micronodules	–	–	–	–	TR	TR
Carbonate unspec.	–	–	2	3	–	–
Foraminifers	10	10	5	8	–	–
Calc. nannofossils	50	40	40	40	10	10
Diatoms	30	40	40	35	TR	TR
Radiolarians	5	5	7	8	–	–
Sponge spicules	2	3	1	2	–	–
Silicoflagellates	1	TR	2	1	TR	
Discoasters	TR	–	TR	TR	–	–

CARBON-CARBONATE (%)

	3, 93–95
Organic Carbon	1.49
Total Carbonate	57.0

SITE 510 HOLE CORE 8 CORED INTERVAL 111.5–114.5 m

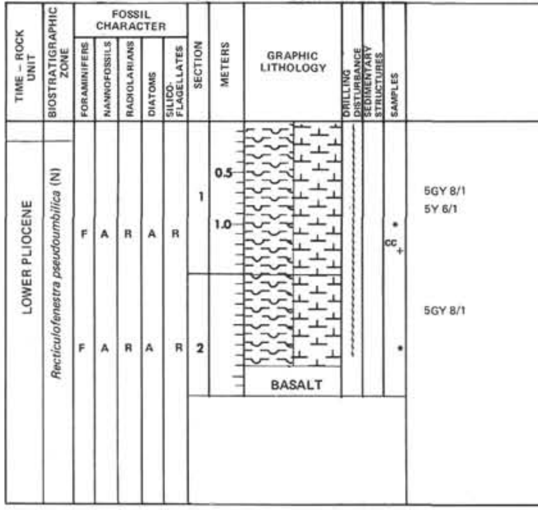

LITHOLOGIC DESCRIPTION

DIATOM-NANNOFOSSIL OOZE

Light greenish gray diatom-nannofossil ooze. Two patches of olive gray ooze in Section 1 at 94–96 cm and 144–150 cm. No other structures seen due to intense drilling disturbance. Odor of H_2S when sections were split. Basalt was recovered in the bottom of Section 2. The individual pieces are described in the igneous rock core barrel summaries.

SMEAR SLIDE SUMMARY (%)

	1-99	2-76
COMPOSITION:		
Volcanic glass (light)	TR	TR
Carbonate unspec.	3	4
Foraminifers	5	5
Calc. nannofossils	45	40
Diatoms	40	40
Radiolarians	5	8
Sponge spicules	2	TR
Silicoflagellates	1	1

CARBON-CARBONATE (%)

	1, 121–123
Organic Carbon	0.90
Total Carbonate	61.0

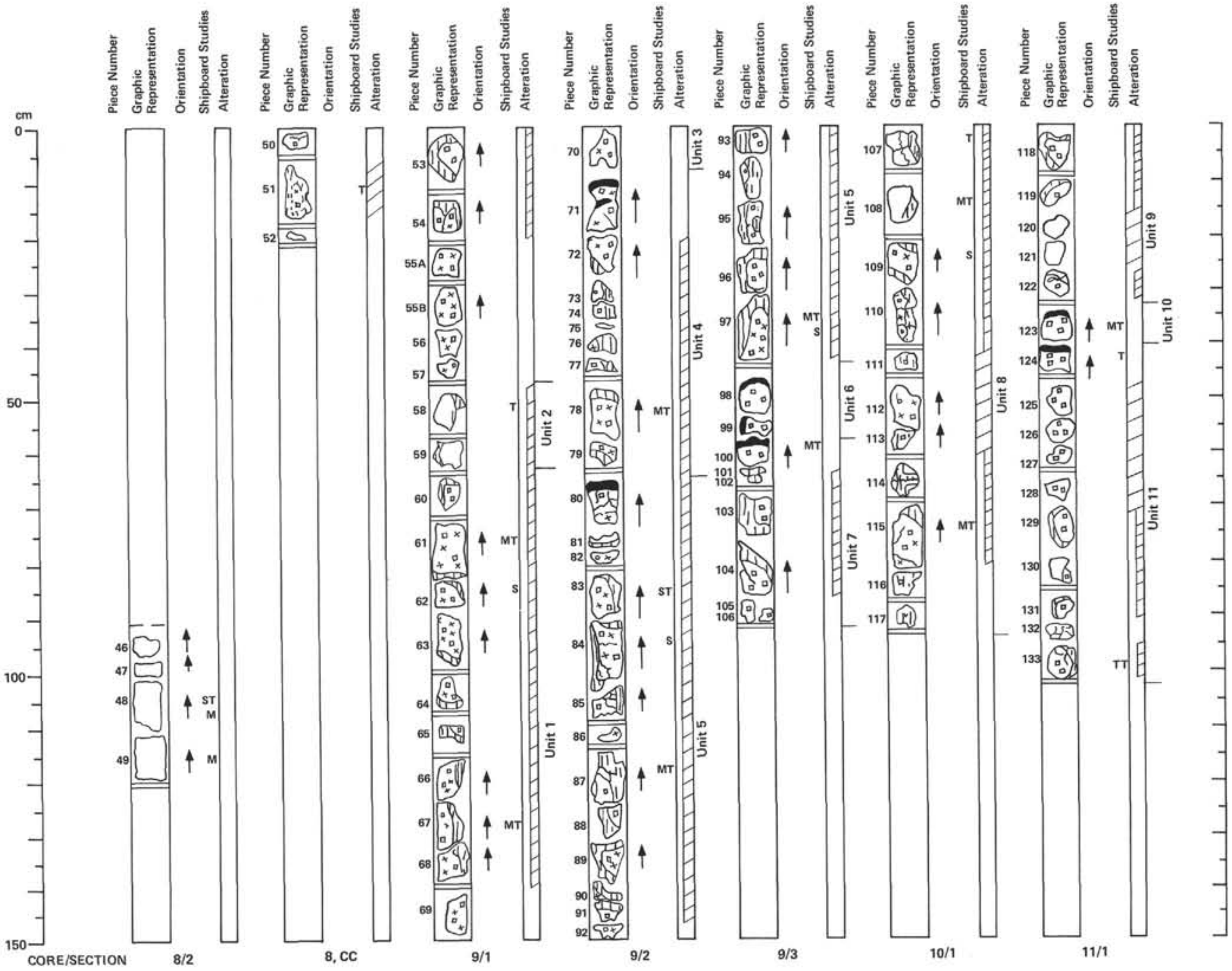

70-510-8 through 11 Depth: 2907.0–2928.0 m (111.5–132.5 mBSF)

8-2, Piece 46–9-1, Piece 58 (Unit 1)

Dominant Lithology: Moderately plagioclase clinopyroxene phyric basalt.

Macroscopic Description: Medium-grained, moderately plagioclase-clinopyroxene phyric basalt. Phenocrysts are from 1–5 mm in length. Alteration rinds are present. Numerous tiny, irregularly shaped voids, often coated with a blue clay are present. Other voids are filled with green smectite. The filled voids are associated and found in the alteration rinds.

Thin Section Descriptions

8-2, 100–102 cm (Piece 48):

Name: Medium-grained moderately plagioclase phyric basalt (flow interior)

Texture: Intersertal to hyaloophitic – glass phase showing quenched texture

Phenocrysts: Olivine, 1%, 0.4x0.4 mm, euhedral; plagioclase, 12%, 5.0x3.0 mm, euhedral

Groundmass: Plagioclase, 30%, 0.4x0.008 mm, microlites; clinopyroxene, 10%, 0.04 mm, anhedral; magnetite, 7%, < 0.008 mm, skeletal; plagioclase and pyroxene, 40%, < 0.008 mm, sheal-like clusters

Alteration: Smectite – green and brown, iddingsite and talc replacing olivine

8-2, 104–106 cm (Piece 48):

Name: Moderately plagioclase-olivine phyric basalt

Texture: Hyalopilitic

Phenocrysts: Olivine, 1–2%, 0.2x0.2 mm; plagioclase, 7–10%, 0.6x0.4–1.2x0.8 mm; blocky, euhedral

Groundmass: Plagioclase, 20–25%, 0.36x0.06 mm, skeletal laths; magnetite, 8%, skeletal; glass, 60%, pyrite, ~ 3%, secondary veins

Alteration: Smectite, 8–10% replacing glass; talc and iddingsite, 1–2%, pseudomorphs after olivine

8, CC, 14–16 cm (Piece 51):

Name: Medium-grained moderately plagioclase phyric basalt (flow interior)

Texture: Hyaloophitic to hyalopilitic

Phenocrysts: Plagioclase, 7%, 1.2x0.8 mm, euhedral

Groundmass: Olivine, 6%, 0.12x0.1 mm, subhedral; plagioclase, 20%, 0.25x0.01 mm, microlites; magnetite, 3%, < 0.008 mm; skeletal; clinopyroxene and plagioclase, 55%, mature sheaf texture

Vesicles: Voids, 3%, filled with smectite, irregular shape

Alteration: Iddingsite and talc, 3%, replacing olivine

9-1, Pieces 58–59 (Unit 2)

Dominant Lithology: Moderately plagioclase-olivine phyric basalt (next to glassy margin)

9-1, 50–52 cm (Piece 58):

Name: Moderately plagioclase-olivine phyric basalt (next to glassy margin)

Texture: Variolitic to hyalopilitic

Phenocrysts: Olivine, < 1%, 0.5x0.5 mm, subhedral; plagioclase, 2–4%, 1.0x2.0 mm, laths

Groundmass: Olivine, 3–4%, 0.06x0.06 mm, anhedral; plagioclase, 10%, 0.6x0.8 mm, skeletal laths; clinopyroxene, 3–4%, 0.02x0.02 mm, anhedral; magnetite, 3–4%; glass, 75%, variolites and microlites; pyrite, 1%, anhedral-subhedral

Vesicles: 2%, 0.3 mm

Alteration: Pyrite scattered replacing glass and magnetite

9-1, Piece 60–9-2, Piece 70 (Unit 3)

Dominant Lithology: Medium-grained moderately to highly plagioclase phyric basalt.

Macroscopic Description: Medium-grained moderately to highly plagioclase phyric basalt. Large plagioclase phenocrysts are present. Alteration rims (5–10 mm thick) are common with associated voids filled with smectite and blue clay mineral.

Thin Section Descriptions

9-1, 76–79 cm (Piece 61):

Name: Medium-grained highly plagioclase phyric basalt (flow interior)

Texture: Hyalopilitic

Phenocrysts: Plagioclase, 20%, 2.0x1.0 mm, euhedral

Groundmass: Olivine(?), 7%, 0.08x0.08 mm, euhedral to subhedral; plagioclase, 20%, 0.25x0.15 mm, microlites; clinopyroxene, 2%, 0.04 mm, anhedral; magnetite, 5%, 0.01 mm, skeletal; pyroxene and plagioclase, 45%, < 0.008 mm, immature variolitic texture.

Alteration: Pale brown clay replacing olivine

9-1, 122–125 cm (Piece 67)

Name: Medium-grained moderately plagioclase phyric basalt (flow interior)

Texture: Hyalopilitic-subophitic

Phenocrysts: Plagioclase, 7%, 1.0x0.5 mm and 0.5x0.2 mm, euhedral

Groundmass: Olivine, 6%, 0.16x0.1 mm, anhedral to subhedral; plagioclase, 35%, 0.4x0.01 mm, microlites; clinopyroxene, 3%, 0.1x0.005 mm, anhedral; magnetite, 4%, 0.01 mm, skeletal, glass, 45% mature sheaf texture

9-2, Pieces 71–79 (Unit 4)

Dominant Lithology: Medium-grained highly plagioclase phyric basalt.

Macroscopic Description: Medium-grained highly plagioclase phyric basalt to fine-grained glassy basalt. In all pieces the feldspars found in the alteration rinds are coated with a green mineral. Vugs are coated and filled with blue-green smectite.

Thin Section Description

9-2, 52–55 cm (Piece 78):

Name: Medium-grained highly plagioclase phyric basalt (flow interior)

Texture: Hyaloophitic

Phenocrysts: Plagioclase, 12%, 2.0x0.8 mm, euhedral

Groundmass: Olivine, 8%, 0.12x0.12 mm, euhedral; plagioclase, 22%, 0.25x0.01 mm, microlites; clinopyroxene, 3%, 0.04x 0.02 mm, anhedral; magnetite, 5%, < 0.008 mm; glass, 50%, mature sheaf texture

Alteration: Talc and iddingsite(?), 8% replacing olivine; smectite, 2% around olivine

9-2, Piece 80–9-3, Piece 97 (Unit 5)

Dominant Lithology: Moderately to highly plagioclase-olivine phyric basalt.

Macroscopic Description: Glassy to fine-grained moderately to highly plagioclase-olivine phyric basalt. Many hairline cracks and fractures occur which are filled with blue green clay. Alteration rinds are present throughout with green (chlorite? or smectite?) coatings on plagioclase phenocrysts in these zones.

Thin Section Descriptions

9-2, 80–83 cm (Piece 83):

Name: Moderately to highly plagioclase-olivine phyric basalt (next to glassy margin)

Texture: Hyalopilitic

Phenocrysts: Olivine, 1%, 0.18x0.20 mm, subhedral; plagioclase, 10%, 0.8x0.7 to 1.5x1.2 mm, blocky to lathy

Groundmass: Plagioclase, 30%, 0.7x0.08 mm, skeletal laths; magnetite, 7%, 0.005–0.010 mm, skeletal; glass, 50%, plumose plagioclase-clinopyroxene groups

Alteration: Talc and iddingsite(?), pseudomorphs after olivine; clays, 10%, in voids, replacing glass and in veins; Fe-oxide, 1%, in smectite veins

9-2, 120–123 cm (Piece 87):

Name: Medium-grained moderately plagioclase-olivine phyric basalt (flow interior)

Texture: Hyaloophitic

Phenocrysts: Olivine, 1%, 0.7x0.3 mm, euhedral; plagioclase, 7%, 0.7x0.25 mm

Groundmass: Olivine, 6%, 0.15x0.10 mm, subhedral; plagioclase, 30%, 0.32x0.01 mm, microlites; clinopyroxene, 2%, 0.025x 0.01 mm, anhedral; magnetite, 4%. < 0.008 mm; skeletal; glass, 55%, mature sheaf texture.

Vesicles: Voids, 1%, 0.01 mm, scattered, irregular and filled with green smectite

Alteration: Smectite in fractures and replacing glass; Fe-hydroxides and iddingsite, 7%, replacing olivine

9-3, 39–42 cm (Piece 97):

Name: Medium-grained moderately plagioclase phyric basalt (flow interior)

Texture: Hyaloophitic to hyalopilitic

Phenocrysts: Plagioclase, 7%, 1.2x0.6 mm, euhedral

Groundmass: Olivine, 3%, 0.2x0.05 mm, subhedral; plagioclase, 20%, 0.8x0.008 mm, microlites; magnetite, 4%, < 0.008 mm, skeletal; plagioclase and pyroxene, 64%, < 0.008 mm, sheaf-like clusters of crystals due to quenching

Alteration: Smectite, 1%, scattered, replacing glass; iddingsite(?) around or in fractures of olivine crystals

9-3, Pieces 98–99 (Unit 6)

Dominant Lithology: Very fine-grained moderately plagioclase phyric basalt

Macroscopic Description: Very fine-grained moderately plagioclase phyric basalt. All fragments have glassy rinds. Feldspar phenocrysts are altered as evidenced by a green mineral (smectite? or chlorite?) coating.

9-3, Pieces 100–106 (Unit 7)

Dominant Lithology: Moderately plagioclase phyric basalt.

Macroscopic Description: Medium-grained moderately plagioclase phyric basalt. Piece 100 represents top of a flow unit. Alteration rinds are common with blue and/or green clay coatings on broken faces.

Thin Section Description

9-3, 53–59 cm (Piece 100):

Name: Moderately plagioclase phyric basalt (glassy margin)

Texture: Variolitic

Phenocrysts: Olivine, <1%, 0.24x0.24 mm, euhedral, plagioclase, 8–10%, blocky euhedra

Groundmass: Olivine, 3–5%, 0.06x0.06 mm, euhedral; plagioclase, 7–10%, 0.36x0.02 mm, acicular; magnetite, 3–4%, skeletal; glass, 70%, variolites

10-1, Pieces 107–117 (Unit 8)

Dominant Lithology: Moderately plagioclase phyric basalt

Macroscopic Description: Fine- to medium-grained plagioclase phyric basalt. Alteration occurs in every piece. Vesicles and primary voids are filled with blue or green smectite. Within the alteration rinds the plagioclase crystals are coated with a green clay. The alteration is controlled by fracture patterns.

Thin Section Descriptions

10-1, 4–6 cm (Piece 107):

Name: Moderately plagioclase phyric basalt (next to glassy margin)

Texture: Hyalopilitic to variolitic

Phenocrysts: Olivine, < 1%, 0.4x0.4 mm, anhedral; plagioclase, 2%, 0.6x0.15 mm, laths

Groundmass: Olivine, 5%, 0.06x0.06 mm, anhedral; plagioclase, 15%, 0.36x0.06 mm, skeletal laths; clinopyroxene, 5%, 0.04x 0.04 mm, anhedral; magnetite, 5–8%, skeletal; glass 70%, mature sheafs and plumose clinopyroxene, plagioclase and olivine

Vesicles: 1%, 0.5 mm, empty, ovoid

Alteration: Pyrite, 3–5%, vein mineral, also replacing magnetite and glass

10-1, 14–18 cm (Piece 108) :

Name: Moderately plagioclase-phyric basalt (glassy margin)

Texture: Variolitic

Phenocrysts: Olivine, <1%, 0.3x0.2 mm, subhedral; plagioclase, 4–7%,0.6x0.12 mm subequant to euhedral laths

Groundmass: Olivine, 5–8%, 0.1x0.1 mm, skeletal to blocky; plagioclase, 8–10%, 0.36x0.08 mm, skeletal laths; magnetite, 5%, 0.012 mm, skeletal; glass, 70–80%, represented by variolites

10-1, 73–75 cm (Piece 115):

Name: Medium-grained moderately plagioclase phyric basalt (flow interior)

Texture: Intersertal

Phenocrysts: Plagioclase, 7%, 0.8x0.5 mm, euhedral or subhedral laths

Groundmass: Olivine, 3%, subhedral; plagioclase, 40%, 0.3x0.008 mm, microlites; clinopyroxene, 27%, 0.08x0.04 mm, anhedral; magnetite, 3%, < 0.005 mm, skeletal; plagioclase and pyroxene, 20%

Alteration: Calcite, 1%, brown smectite, 10–15%, replacing glass and filling voids

11-1, Pieces 118–122 (Unit 9)

Dominant Lithology: Moderately plagioclase phyric basalt.

Macroscopic Description: Medium-grained moderately plagioclase phyric basalt. Numerous vesicles and irregularly shaped voids are filled by blue or green clay. Phenocrysts of feldspars are altered as evidenced by presence of green clay coating.

11-1, Piece 123 (Unit 10)

Dominant Lithology: Fine-grained moderately plagioclase phyric basalt.

Macroscopic Description: Fine-grained moderately plagioclase phyric basalt. Fractures are present. Phenocrysts of feldspars occur in glassy areas as well as non-glassy zones.

Thin Section Description

11-1, 36–39 cm (Piece 123):

Name: Fine-grained, moderately plagioclase phyric basalt (next to glassy margin)

Texture: Sub-glomerophyric with groundmass hyalopilitic

Phenocrysts: Plagioclase 10%, 0.8x0.4 mm, euhedral

Groundmass: Olivine, 7%, 0.15x0.08 mm, subhedral; palgioclase, 12%, 0.24x0.05 mm, microlites; clinopyroxene, 5%, 0.15x 0.08 mm, euhedral, magnetite, 3%, < 0.008 mm skeletal; glass, 60% immature variolitic texture

Alteration: Smectite, 3%, filling fractures and replacing glass and some olivine

11-1, Pieces 124–133 (Unit 11)

Dominant Lithology: Moderately plagioclase phyric basalt.

Macroscopic Description: Fine- to medium-grained moderately plagioclase phyric basalt.Piece 124 represents the top of a flow. Vesicles and voids are filled with blue or green clay. Plagioclase phenocrysts are altered and show green mineral coatings (chlorite? or smectite?). The alteration is related to the fracturing.

Thin Section Description

11-1, 40–43 cm (Piece 124):

Name: Fine-grained moderately plagioclase phyric basalt (next to glassy margin)

Texture: Glomerophyric with variolitic groundmass

Phenocrysts: Plagioclase, 10%, 2.0x0.7 mm, euhedral

Groundmass: Olivine, 3%, 0.15x0.10 mm, euhedral; plagioclase, 7%, 0.4x0.015 mm, microlites; clinopyroxene, 5%, 0.15x0.10 mm, anhedral; magnetite, 2%, < 0.004 mm, skeletal; glass, 73%, variolitic

Alteration: Smectite replacing olivine, and fractures, iddingsite, talc replacing olivine

11-1, 98–100 cm (Piece 133)

Name: Medium-grained moderately plagioclase phyric basalt (flow interior)

Texture: Intersertal

Phenocrysts: Plagioclase, 8%, 1.5x1.0 mm, euhedral twinned crystals

Groundmass: Plagioclase, 36%, 0.3x0.008, microlites; clinopyroxene and plagioclase, 50%, < 0.008 mm, sheaf-like, intergrowths; magnetite, 3–4%, 0.01 mm, skeletal

Vesicles: Voids, 2%, filled with colorless and brown clay

Alteration: Clays (colorless and brown) replacing olivine

11-1, 98–100 cm (Piece 133):

Name: Moderately plagioclase-olivine phyric basalt (next to glassy margin)

Texture: Hyalopilitic to variolitic

Phenocrysts: Olivine, 5%, 0.24x0.24 mm, rounded to euhedral plagioclase, 5%, 1.7x1.2 mm, blocky

Groundmass: Olivine, 5%, 0.05x0.05 mm, blocky; plagioclase, 20%, 0.08x0.7 mm, skeletal to acicular; magnetite, 5%, ilmenite, 60%, sheafs of clinopyroxene and plagioclase

Alteration: Iddingsite and talc, < 1% replacing olivine, smectite, 8–10% replacing glass and found in voids

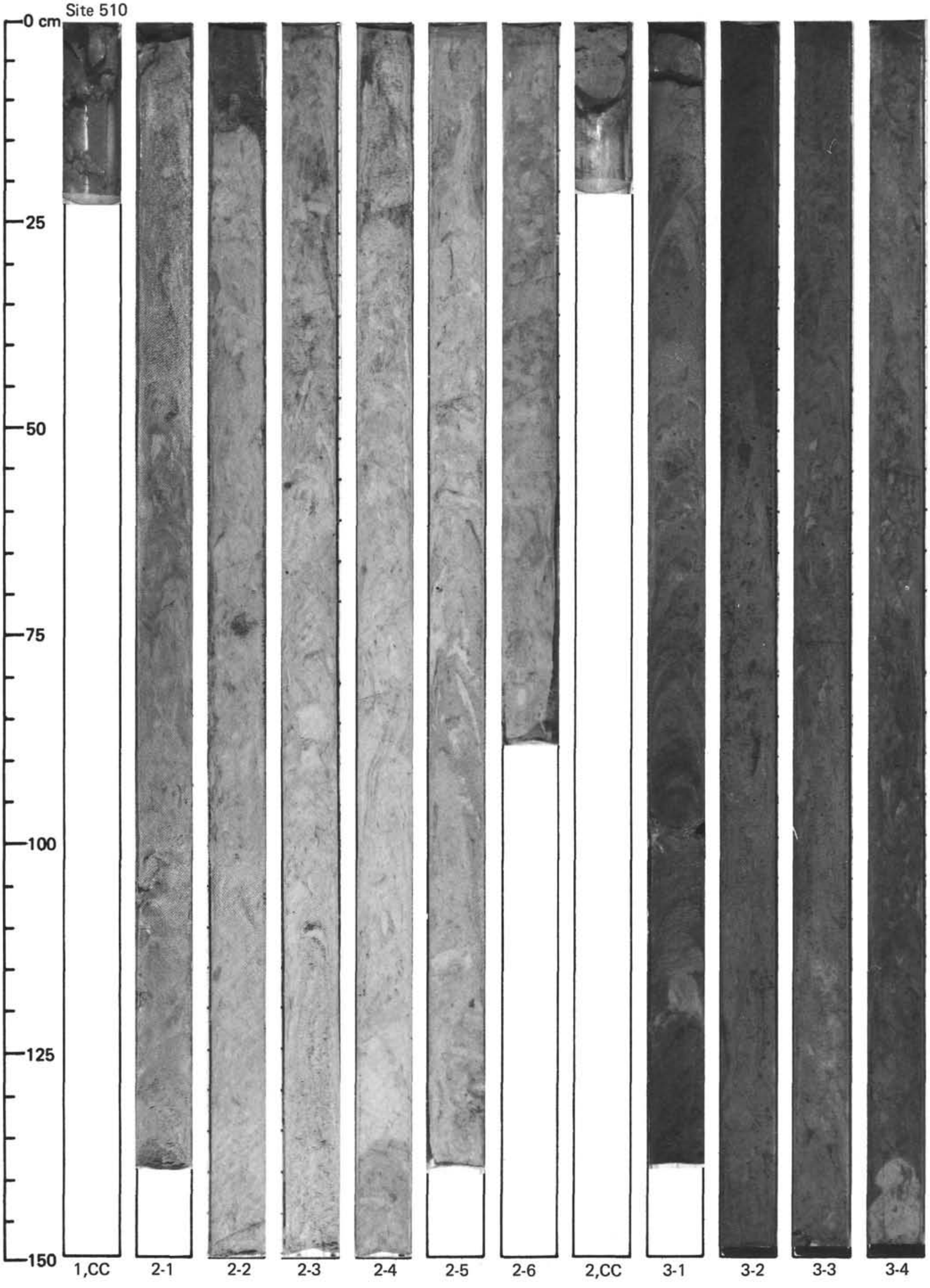
Site 510
0 cm
25
50
75
100
125
150
1,CC
2-1
2-2
2-3
2-4
2-5
2-6
2,CC
3-1
3-2
3-3
3-4

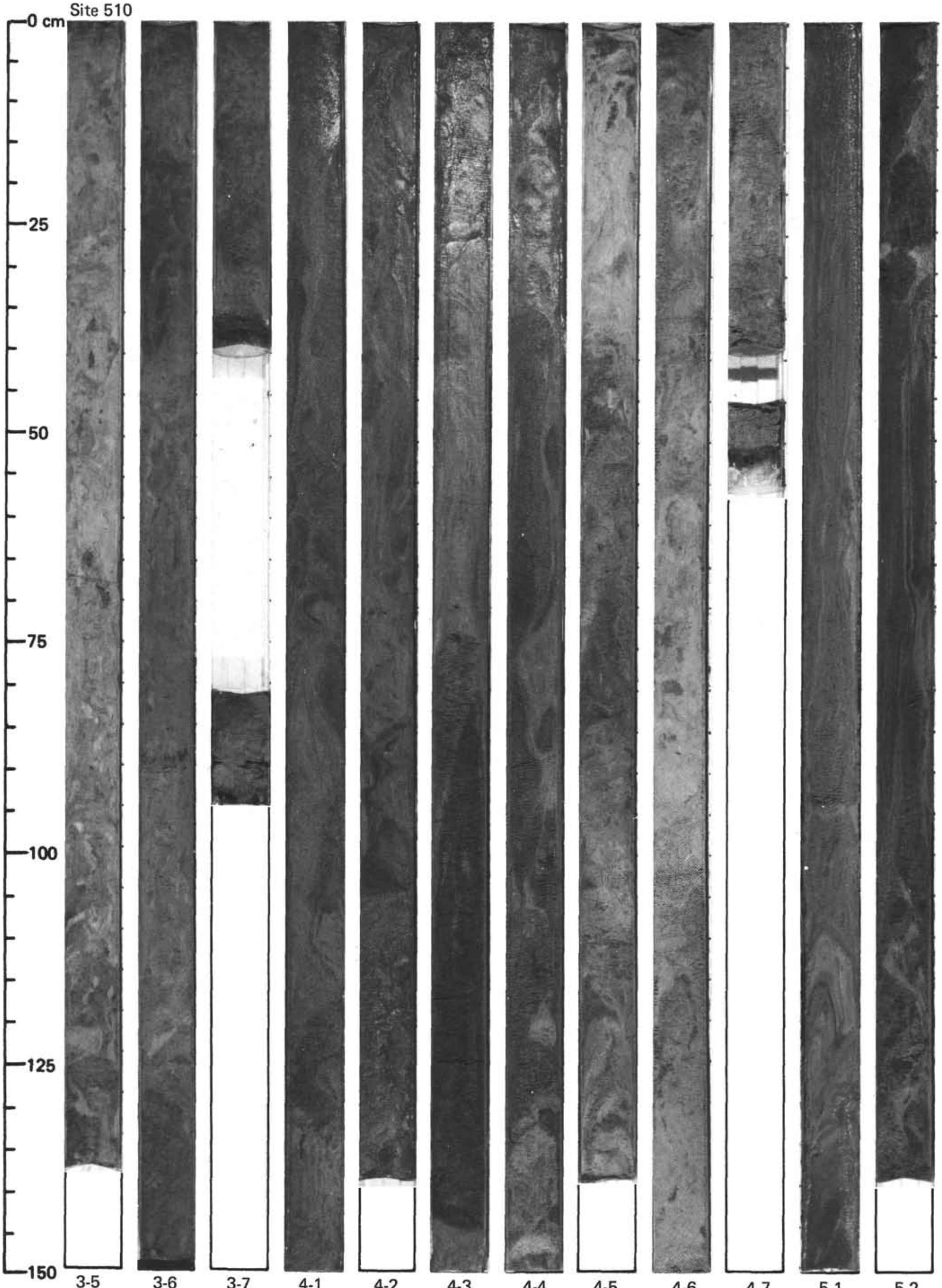
Site 510
0 cm
25
50
75
100
125
150
3-5
3-6
3-7
3,CC
4-1
4-2
4-3
4-4
4-5
4-6
4-7
4,CC
5-1
5-2

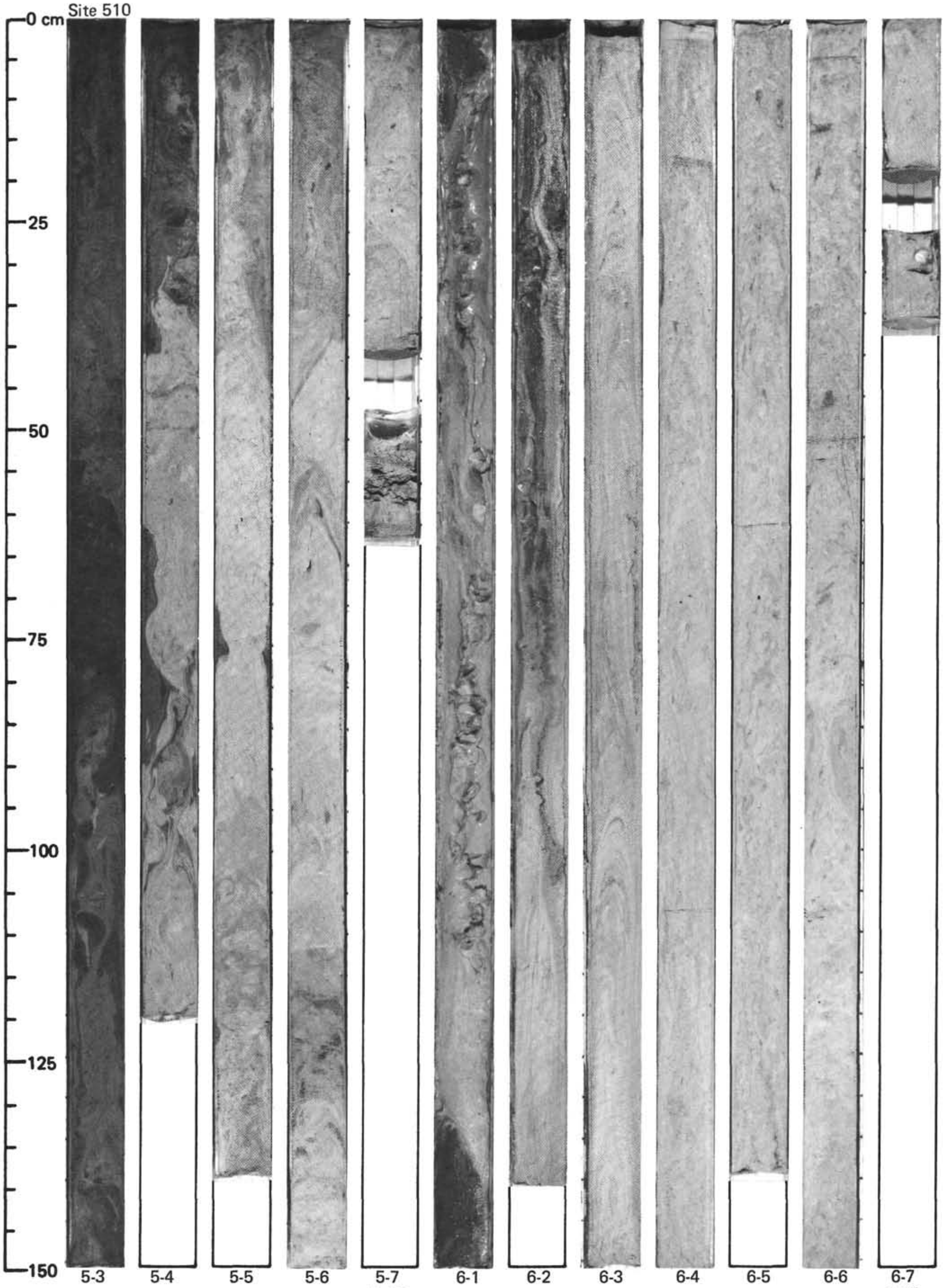
Site 510
0 cm
25
50
75
100
125
150
5-3
5-4
5-5
5-6
5-7
5,CC
6-1
6-2
6-3
6-4
6-5
6-6
6-7
6,CC

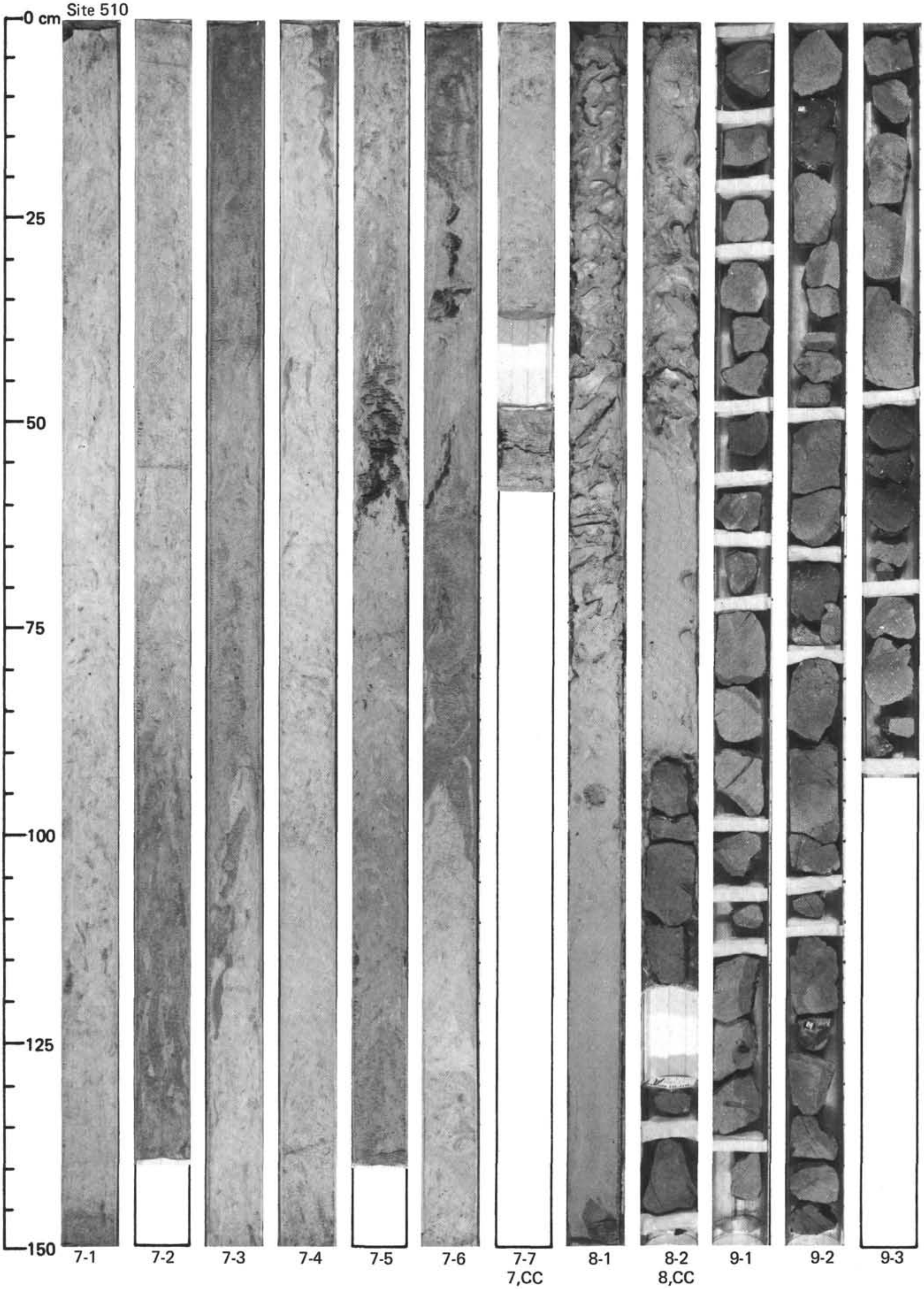
0 cm
Site 510
25
50
75
100
125
150
7-1
7-2
7-3
7-4
7-5
7-6
7-7
7,CC
8-1
8-2
8,CC
9-1
9-2
9-3

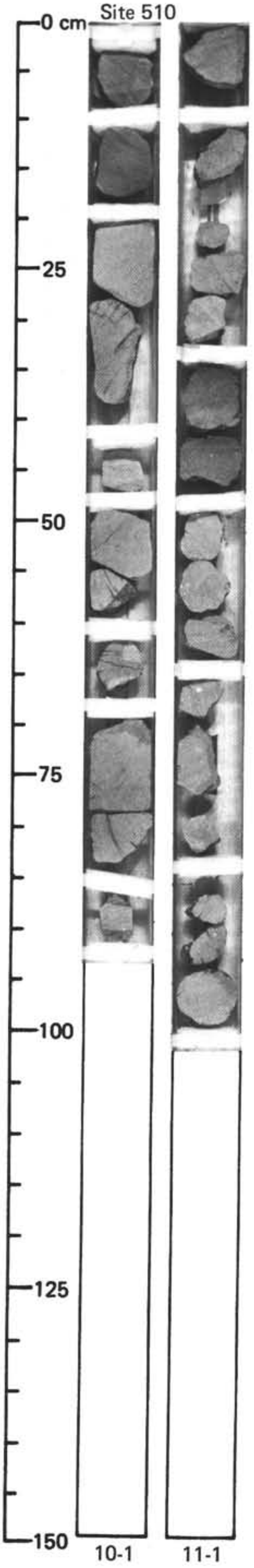
0 cm
25
50
75
100
125
150
Site 510
10-1
11-1